

# Environments of Northeast U.S. Severe Thunderstorm Events from 1999 to 2009

MELISSA M. HURLBUT AND ARIEL E. COHEN

*NOAA/NWS/NCEP/Storm Prediction Center, Norman, Oklahoma*

(Manuscript received 2 May 2012, in final form 14 December 2012)

## ABSTRACT

An investigation of the environments and climatology of severe thunderstorms from 1999 through 2009 across the northeastern United States is presented. A total of 742 severe weather events producing over 12 000 reports were examined. Given the challenges that severe weather forecasting can present in the Northeast, this study is an effort to distinguish between the more prolific severe-weather-producing events and those that produce only isolated severe weather. The meteorological summer months (June–August) are found to coincide with the peak severe season. During this time, 850–500- and 700–500-hPa lapse rates, mixed layer convective inhibition (MLCIN), and downdraft convective available potential energy (DCAPE) are found to be statistically significant in discriminating events with a large number of reports from those producing fewer reports, based on observed soundings. Composite synoptic pattern analyses are also presented to spatially characterize the distribution of key meteorological variables associated with severe weather events of differing magnitudes. The presence of a midlevel trough and particular characteristics of its tilt, along with an accompanying zone of enhanced flow, are found in association with the higher-report severe weather events, along with cooler midlevel temperatures overlaying warmer low-level temperatures (i.e., contributing to the steeper lapse rates). During the meteorological fall and winter months (September–February), large-scale ascent is often bolstered by the presence of a coupled upper-level jet structure.

## 1. Introduction and background

Forecasting deep, moist convection in the northeastern United States presents a unique challenge, as convective initiation, storm coverage, and expected severity of thunderstorms have numerous societal, financial, and workload impacts in one of the most densely populated areas of the country encompassing Pennsylvania, New Jersey, New York, Connecticut, Rhode Island, Massachusetts, Vermont, New Hampshire, and Maine (Fig. 1). A varied landscape that offers a number of lakes and mountains, as well as ocean access, leads to a propensity for outdoor activity, coinciding with the peak severe season in June–August. Large cities are especially vulnerable to thunderstorms, which can threaten millions of people in a relatively small geographical area, cripple public transportation, and lead to widespread power outages. Effects on aviation can be high impact as well, with flight delays and reroutes often necessary, leading to disruptions in air travel as major

airports are affected (Evans et al. 2004). Therefore, accurately depicting the threat is important from an operational forecasting standpoint impacting proper preparations for impending thunderstorms.

Other studies have yielded in-depth investigations of the nature of convection, including severe convection across the northeastern United States (e.g., Lombardo and Colle 2010; Lombardo and Colle 2011; Murray and Colle 2011). Both Lombardo and Colle (2010) and Lombardo and Colle (2011) set out to identify characteristics unique to northeastern United States convection. Lombardo and Colle (2010) considered measures of buoyancy, depictions of synoptic and mesoscale forcing, and the spatiotemporal distribution of convective initiation among a variety of convective modes and organizational–morphological traits for convection. Murray and Colle (2011) used a similar approach to develop a climatology of northeastern United States convection. Likewise, Lombardo and Colle (2011) compared these similar characteristics for severe thunderstorms, including a focus on specific severe storm hazards emanating from the various convective modes.

Additionally, previous research has shown that local effects influence storm development and severity (e.g.,

---

*Corresponding author address:* Melissa Hurlbut, Storm Prediction Center, 120 David L. Boren Blvd., Norman, OK 73072.  
E-mail: melissa.hurlbut@noaa.gov

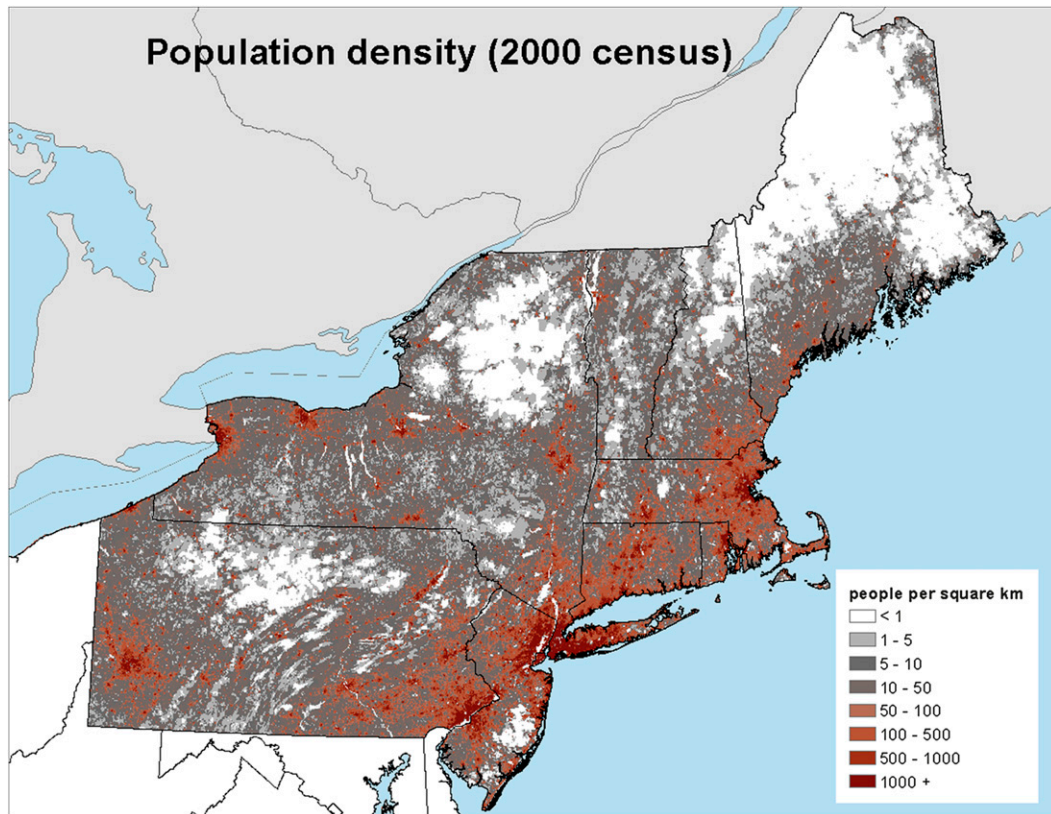


FIG. 1. Population density of the Northeast in 2000 census.

Bosart et al. 2004; LaPenta et al. 2005; Lericos et al. 2007; Riley and Bosart 1987; Wasula et al. 2002), such as marine (lake and ocean) and terrain variations, and the orientation of favored river valleys. These various surface features may provide locally modified low-level winds and associated bolstering of low-level shear (Bosart et al. 2004), in addition to sources of enhanced surface convergence and upward motion, such as sea- or lake-breeze boundaries, and upslope flow. Despite the mesoscale influences of inhomogeneous surface conditions across the northeast United States, we focus attention on the larger-scale upper-air patterns and statistical analysis of derived parameters therein as indicators of a potential severe weather event.

Furthermore, a higher number of severe reports are collocated with the greater population densities of Pittsburgh and Philadelphia, Pennsylvania; New York City, New York; and surrounding coastal areas of New Jersey; Long Island, New York; and New England (Fig. 2) (Doswell et al. 2005). However, for the purposes of this study, all severe thunderstorm reports are treated independently from variations in population. Although it is understood that a greater number of reports was likely recorded near the more populated corridors, no

attempt was made to normalize these reports (Anderson et al. 2007).

As the aforementioned studies focus only on the warm season, we attempt to expand the climatological analysis of northeastern United States to encompass severe thunderstorm environments throughout all seasons. In this endeavor, we try to expand this investigation over a broad range of large-scale patterns, as well as a relatively larger suite of variables derived from observed soundings. Furthermore, we test these variables for statistical significance in distinguishing between various severe report quantities.

## 2. Data and methodology

The objective of this study is to stratify the synoptic regimes and related thermodynamic and kinematic environments that most commonly favor severe thunderstorm events resulting in large numbers of reports, and to compare these characteristics with those associated with a small number of reports. National Weather Service definitions for severe weather [i.e., thunderstorms producing hail of at least 2.54 cm (1 in.) in diameter, winds of at least  $25.7 \text{ m s}^{-1}$  (50 kt), or a tornado] were

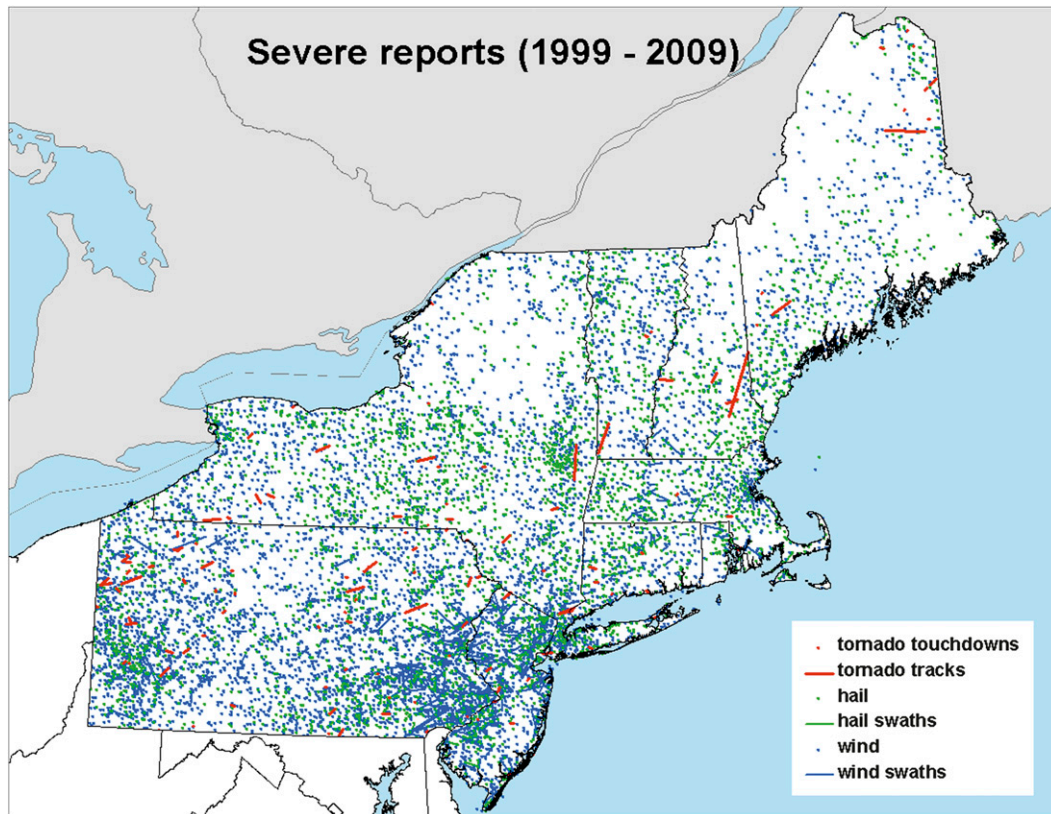


FIG. 2. All severe reports from 1999 to 2009 in the Northeast.

used in order to develop a severe weather climatology that can be effectively applied to convective forecasting.

Hail sizes of less than 2.54 cm (1 in.) in diameter were excluded from the analysis in accordance with the latest National Weather Service severe thunderstorm criteria (as of 5 January 2010) in order to assess environments and patterns that can be applied to convective forecasts, despite the criterion of 1.9 cm (0.75 inch) that was valid during the study period. Significant thunderstorm events were also cataloged [i.e., hail  $\geq 5.08$  cm (2 in.) in diameter, thunderstorm wind gusts  $\geq 33.4$  m s<sup>-1</sup> (65 kt, 1 kt = 0.51 m s<sup>-1</sup>), or tornadoes that produced damage rated as at least category 2 on the Fujita-enhanced Fujita scales ( $\geq$ F2–EF2), after Hales (1988)]. During the study period, a maximum of 247 reports were recorded in a single convective day, while a minimum of 1 report was frequently recorded.

Storm Prediction Center (SPC) storm report data for the period from 1999 through 2009 were examined. Preliminary reports are utilized within the Storm Prediction Center to provide instant verification for convective outlooks. As such, the authors had a particular interest in the preliminary dataset in order to apply the results of the study to forecasting an appropriate outlook

category. For the first half of 1999 where preliminary data were unavailable, National Climatic Data Center (NCDC) data were used to supplement the dataset.

For this study, an event was defined as any 24-h period beginning at 1200 UTC in which at least one severe weather report was documented in Pennsylvania, New Jersey, New York, Connecticut, Rhode Island, Massachusetts, Vermont, New Hampshire, and/or Maine. These events were further subdivided into several arbitrary subsets: 10 reports or fewer, 11–50 reports, 51–100 reports, >100 reports, significant wind, and significant hail based on potential workload considerations for forecasters, media, emergency managers, and others affected by the storms (Fig. 3). By removing 0.75-in. hail reports, 40 cases that contained less than five reports per event were deleted from the original dataset, with a subsequent shift in report distributions. Although only a minor affect was noted for the 1–10- and 11–50-report subsets, the total number of reports was primarily reduced in the higher-report datasets, resulting in 22 and 6 fewer events, respectively. While these changes are not insignificant, the authors believe that removing the 0.75-in. hail reports allowed a focus on truly damaging weather events. Furthermore, error may also exist in the

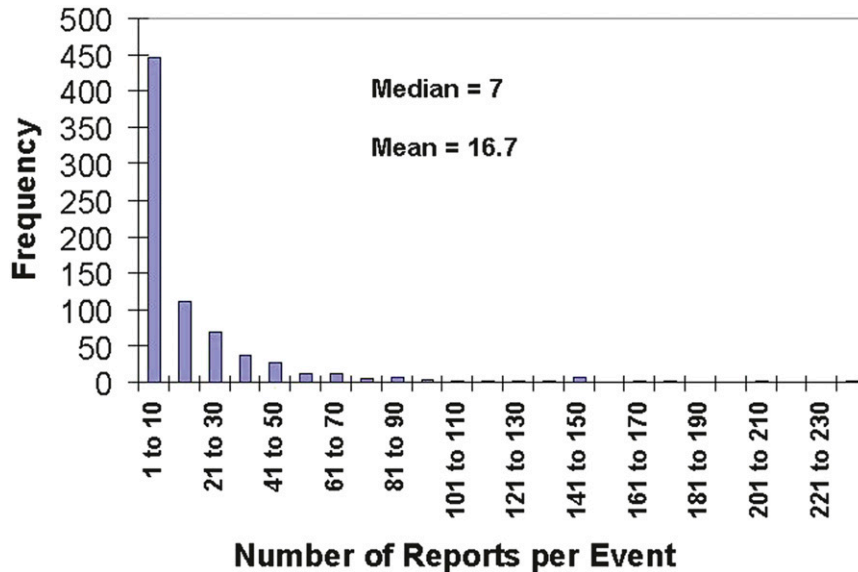


FIG. 3. Frequency of the number of severe reports recorded per event from 1999 to 2009 in the Northeast.

lower-end hail sizes; since solicitation of larger report sizes may not have occurred once a 0.75-in. hail report (formerly verifying the storm warning) was received. As no official studies have been published regarding the effects of the criteria change on hail reports, no further speculation will be offered. Additional information cataloged for each event included the type and number of severe thunderstorm reports (Figs. 4 and 5), time of day for the first report and cessation of the severe event (i.e., time of last report) (Figs. 6 and 7), and any occurrences of significant severe thunderstorms.

Observed proximity soundings created using the Universal Rawinsonde Observation program (Environmental Research Services 2008) were then manually selected on a case-by-case basis for each event by examining the individual soundings in the National Centers Advanced Weather Interactive Processing System Skew-T Hodograph Analysis and Research Program (NSHARP; Hart et al. 1999). Proximity soundings were visually assessed and selected if the observational data existed within a thermodynamic and kinematic environment that would support thunderstorm development. Sounding times

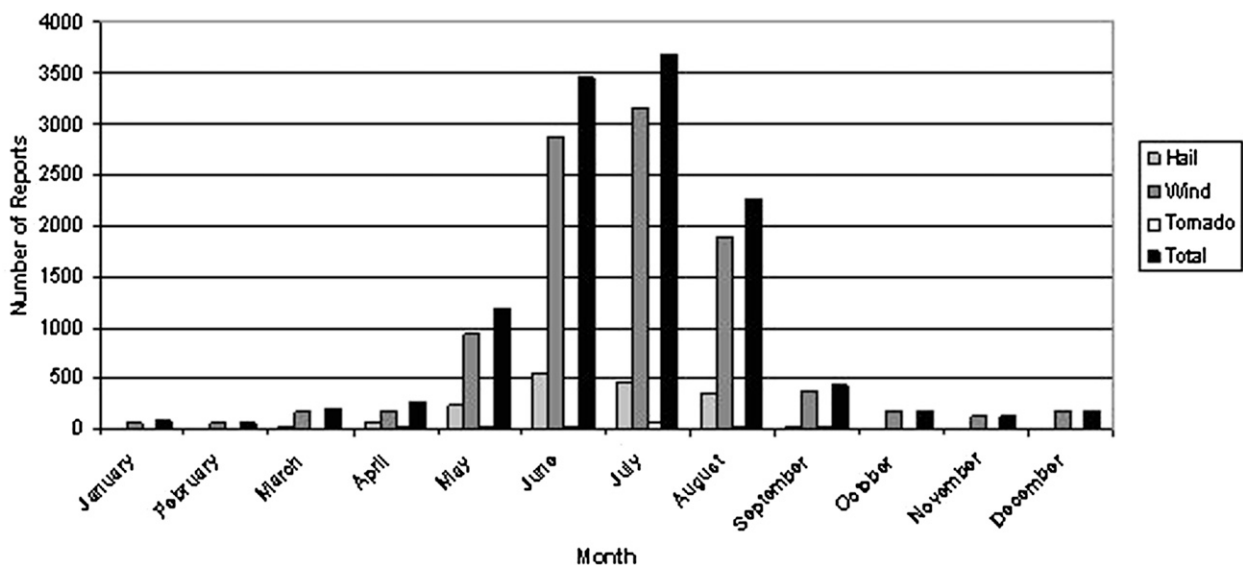


FIG. 4. Number of severe thunderstorm reports by month and type of report from 1999 to 2009 in the Northeast.

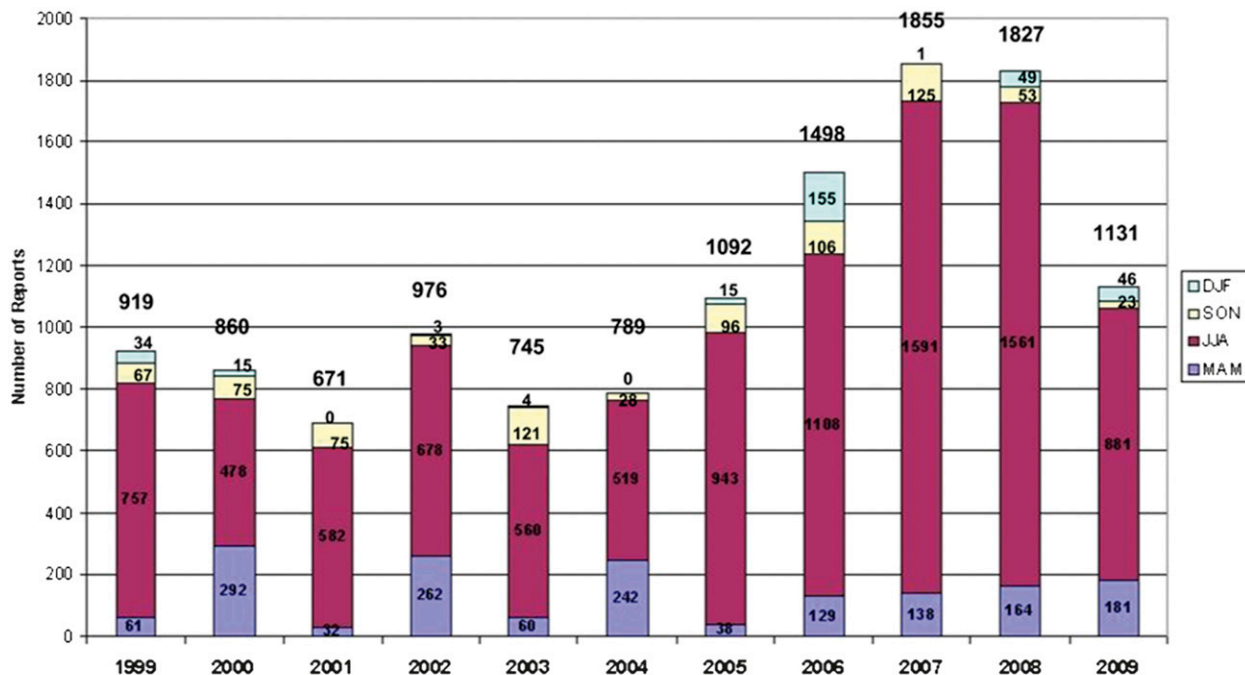


FIG. 5. Number of severe thunderstorm reports by season from 1999 to 2009 in the Northeast.

were chosen to minimize the elapsed time between report times and possible sounding times; that is, reports occurring between 0600 and 1800 UTC warranted 1200 UTC soundings, while reports occurring between 1800 and 0600 UTC involved 0000 UTC soundings (Table 1). Soundings that were deemed to be postfrontal or otherwise unrepresentative due to convective contamination or radiosonde error were rejected from the

analysis. Higher-report days tended to affect a broader area; so on average more soundings were used in these cases (Table 1). Using a National Centers for Environmental Prediction (NCEP) Advanced Weather Interactive Processing System (AWIPS) distance-tracking tool, the distance between the observation site and the farthest reports was measured. The sparseness of the upper-air observations was especially notable across

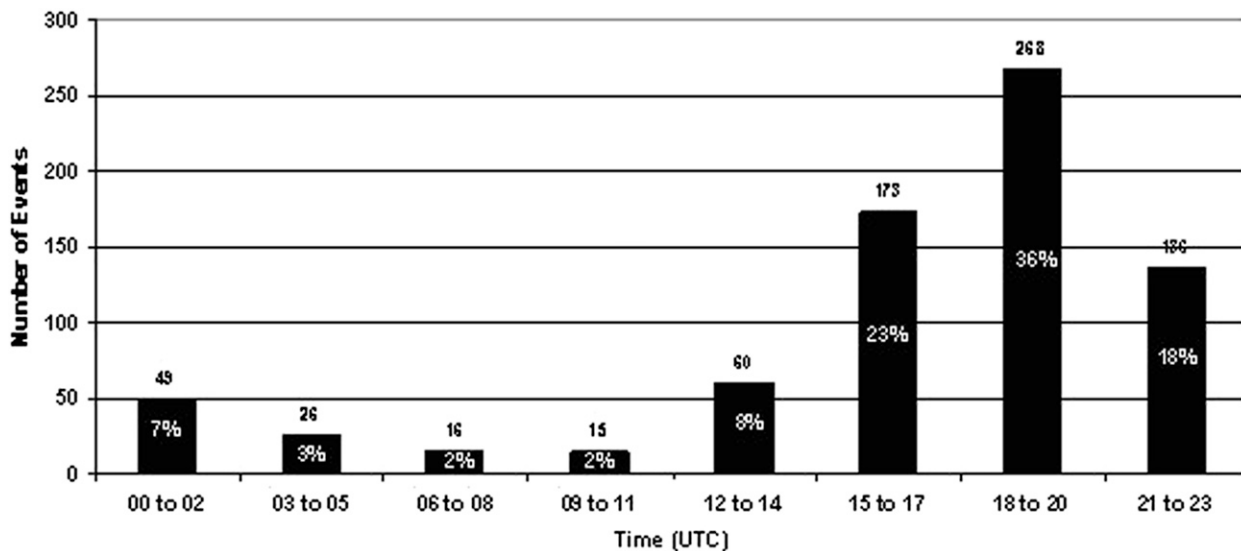


FIG. 6. Diurnal distribution of the time (UTC) of first severe thunderstorm report from 1999 to 2009 in the Northeast.



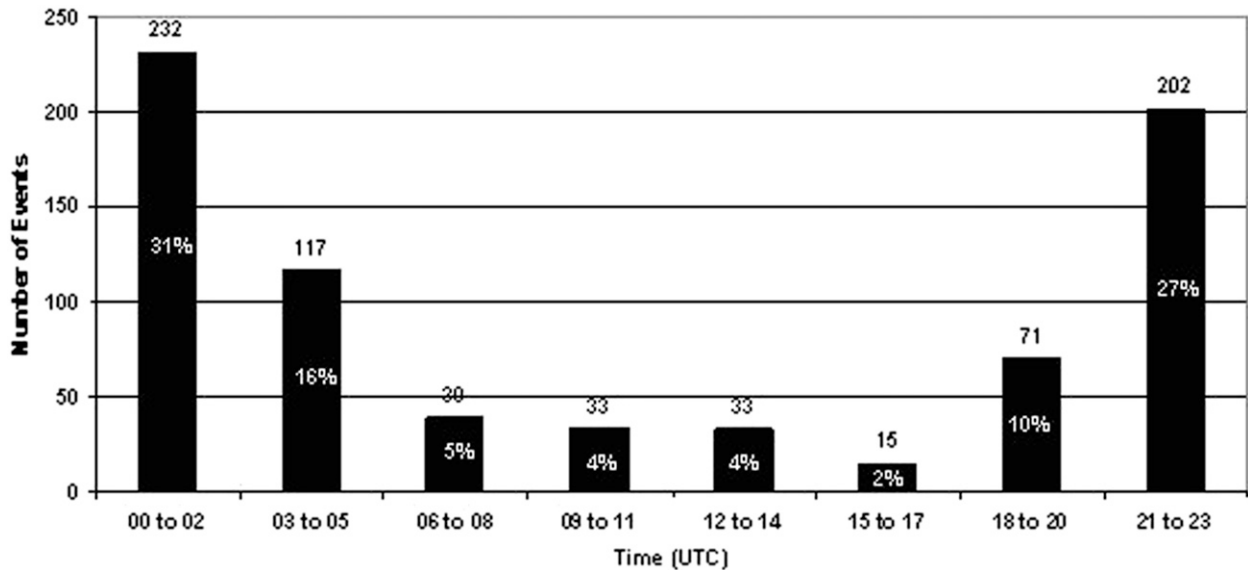


FIG. 7. As in Fig. 6, but for last severe thunderstorm report.

central New York, central and western Pennsylvania, and New Jersey, where, given a west–east-progressing system, there can be up to a 600-km gap between upper-air sites. Nonetheless, soundings were located no more than 250 km (155 mi) from the edges of the report distribution. Although such broad distances can introduce error, especially in the representation of the near-storm environment, we believe that meaningful results can be gleaned from the work, particularly with the large summer dataset.

Additionally, using the North American Regional Analysis (NARR) data at 32-km grid spacing (Mesinger et al. 2006), composite patterns were derived for each report class and for significant severe events based on meteorological seasons. Composite images were created using the same time selections as the upper-air soundings, allowing forecasters to visualize the patterns associated with the observed parameter data.

### 3. Results

#### a. Climatology of events

##### 1) ANNUAL AND MONTHLY FREQUENCY

During the study period, summer (defined as June–August) was found to be the most active season (Figs. 4 and 5), with 498 of 742 (67%) total events occurring in these 3 months. Spring (defined as March–May) is the second-most active season, though with far fewer severe weather days than summer (144 events, or 19% of the total). Fall (defined as September–November) accounted for 75 events (10%), while winter (defined as

December–February) comprised only 3% of the dataset (25 events).

The 14 events with greater than 100 reports (not including hail with size <1 in.) are listed in Table 2. Out of the 11-yr period, the greatest number of reports was recorded in 2007 and 2008, each with similar report

TABLE 1. Proximity sounding count for each event magnitude category on a seasonal basis.

Event reports/type	Season	1200 UTC count	0000 UTC count	Average No. of soundings per event
1–10	Spring	25	62	1.3
	Summer	108	215	1.6
	Fall	15	31	1.3
	Winter	9	7	1
11–50	Spring	25	68	2.7
	Summer	312	534	4.8
	Fall	28	33	2.5
51–100	Spring	2	7	2.3
	Summer	65	121	5.3
101+	Spring	1	4	5
	Summer	39	36	5.8
	Winter	0	2	2
SIGWIND	Spring	1	6	2.3
	Summer	20	45	4.1
	Fall	3	0	3
	Winter	0	9	2.3
SIGHAIL	Spring	8	16	2.7
	Summer	51	75	3.9

TABLE 2. Events with &gt;100 severe reports ranked according to total number of reports.

More than 100 report events excluding hail <1 in.		
1	10 Jun 2008	247
2	2 Jun 2000	201
3	18 Jul 2006	169
4	27 Jun 2007	150
5	19 Jun 2007	150
6	1 Jul 2001	144
7	6 Jul 1999	143
8	6 Jun 2005	141
9	3 Aug 2007	141
10	16 Jun 2008	140
11	1 Dec 2006	126
12	21 Jul 2003	120
13	8 Jun 2007	110
14	11 Jun 2007	110

totals: 1855 and 1827, respectively (Fig. 5). However, as indicated in Table 2, these years were comprised of a few large events, with 387 of these reports occurring over two separate events in 2008, and 441 of these reports occurring in three events for 2007. The year 2006 was the third highest in terms of reports, with the most active winter compared to any other year.

Of the total events, a majority (444 of 742, or 60%), had 10 or fewer reports (Fig. 3). Despite a large dataset of 742 events, only 14 events (2%) from the dataset contained >100 reports (Fig. 3), highlighting the rarity of larger-report events, while the remaining 298 (38%) events recorded between 11 and 100 reports.

## 2) DIURNAL DISTRIBUTION

The peak beginning and end times for the severe weather reports coincide with the diurnal heating cycle, which suggests a large role of insolation in thunderstorm initiation and maintenance. The peak time of the first report is 1900 UTC, with 59% of all first reports occurring between 1500 and 2100 UTC (Fig. 6). Additionally, 18% of first reports are made in the early evening between 2100 and 0000 UTC. First reports infrequently occur in the overnight hours, particularly between 0600 and 1200 UTC when only 4% of first reports occur.

Meanwhile, 58% of last reports are recorded between 2100 and 0300 UTC, with a peak time of last report at 0000 UTC (Fig. 7). The 1500–1700 UTC period is the least likely time for a last report to be made, accounting for 2% of the total.

## 3) SEVERE THUNDERSTORM REPORTS BY TYPE

Severe convective wind is, by far, the predominant severe weather threat for the Northeast (Fig. 4), with 10 161 reports (84%) spanning the 11-yr study period. Hail is the second-most common threat, with 1732 reports

(14%) recorded. Fifty-four out of 742 total events had hail reports that exceeded the total number of wind reports for the corresponding events, or in other words, 7% of the events had a more frequent occurrence of hail than wind. Thus, 93% of events featured predominately wind reports, and damaging wind should be considered the most common severe weather threat in the northeast United States.

Accounting for the past criteria of  $\geq 1.9$ -cm (0.75 in.) hail being considered severe, 2681 reports of 1.9-cm (0.75 in.) hail were made, for a total of 4413 severe hail reports. Even considering this former criterion, only 30% of the database is composed of severe hail reports, once again confirming that damaging wind is the primary severe weather threat across the Northeast.

Tornadoes primarily occurred from May through September, though they rarely occurred in cooler seasons. A total of 190 tornado reports (2%) were collected in the 11-yr study period, with 47 tornado reports having occurred during spring, 115 in summer, 22 in fall, and 6 in winter.

Significant tornadoes occurred infrequently, with one to four F2–EF2s per year with the exception of 2005 when none were recorded. An F3 rating was only recorded in 2003 and 2004, with no higher rating occurring during the study period. However, a sample size of 11 yr is relatively limited for recording more significant events (Weiss et al. 2002). For example, several well-known F3–EF3 tornadoes occurred just prior to and after the study period, including the Mechanicville, New York, F3 event on 31 May 1998 (LaPenta et al. 2005) and more recently an EF3 storm on 1 June 2011 in Springfield, Massachusetts (Banacos et al. 2012). Although they occur at a lesser frequency, violent tornadoes have also been recorded outside the study period, including the well-documented Worcester, Massachusetts, tornado on 9 June 1953, an F4 tornado at Windsor Locks, Connecticut, on 3 October 1979 (Riley and Bosart 1987), and an F5 tornado that struck northwest Pennsylvania in 1985 (Farrell and Carlson 1989).

Interestingly, although severe convective wind is the predominant threat, a greater number of significant hail reports (67) were recorded compared to significant wind incidents (33). It is possible that significant wind occurred more frequently than either anemometer or spotter-estimated reports, with several local storm report annotations being indicative of damage caused by wind speed magnitudes of at least  $33.4 \text{ m s}^{-1}$  (65 kt) (Smith et al. 2010). Other studies have also found significant events to be grossly underestimated with regard to the report density and intensity in *Storm Data*, while relatively less-damaging events were often represented by a larger number of reports (Trapp et al. 2006). Trapp

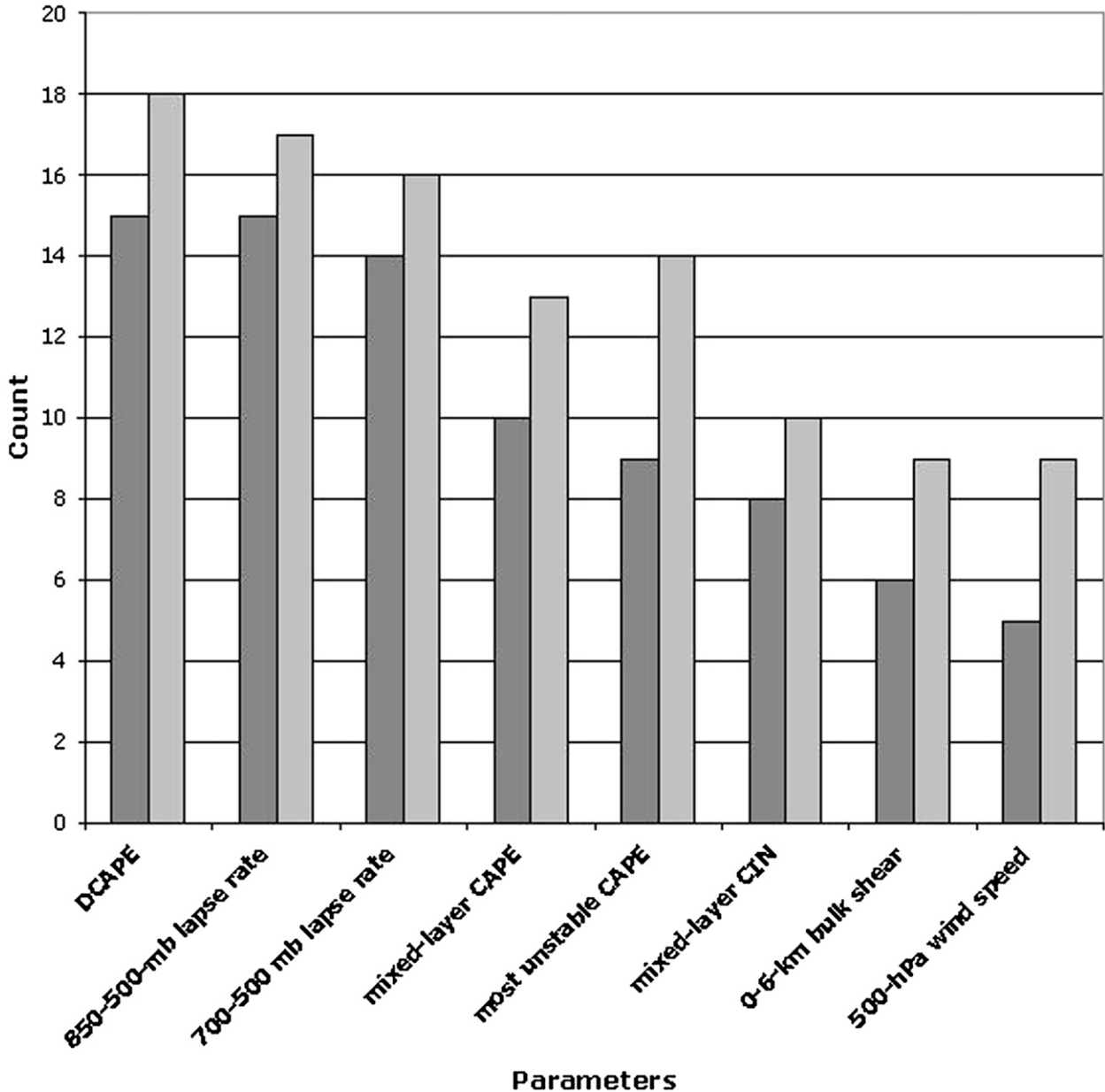


FIG. 8. Number of pairings between which a selection of parameters discriminates at a  $P$  value threshold of 0.05 during the summer.

et al. (2006) also suggested that further solicitation of reports may not occur once a storm warning has been verified, which in turn would affect the *Storm Data* report representation for any given event. Although speculative but perhaps warranting further investigation, other nonmeteorological factors may also contribute to the comparative number of significant events, such as the availability of anemometers and the relative difficulty of estimating wind speeds, whereas hail may be readily measured or compared to an object of similar size.

#### b. Statistical analysis

##### 1) METHODOLOGY

The parameters are grouped into various categories to stratify the dataset subjectively based on impact considerations and event magnitudes. Event categories include the following (herein referred to by parenthetical notation following the category description): 1–10 reports (1–10), 11–50 reports (11–50), 51–100 reports (51–100), at least 101 reports (101+), at least one significant wind report [wind speed of at least  $33.4 \text{ m s}^{-1}$  (65 kt);



TABLE 3. Statistical comparisons (*P* value and mean value) for 850–500-mb lapse rate among various event magnitudes for summer. Comparisons are only provided if the corresponding *P* value is below 0.05.

Pairing of 850–500-hPa lapse rate for 101+ report events with 850–500-hPa lapse rate for number of reports:	<i>P</i> value	Mean value of 850–500-hPa lapse rate ( $^{\circ}\text{C km}^{-1}$ )
1–10	<0.001	6.36
11–50	<0.001	6.41
51–100	<0.001	6.38
101+	N/A	6.77
Sig wind	0.009	6.59

SIGWIND], and at least one significant hail report [hail of at least 5.08-cm (2 in.) diameter; SIGHAIL]. The dataset is further stratified seasonally, owing to the interannual variability in the relative magnitudes of parameters that support severe weather events.

Table 1 provides the number of proximity soundings included within these categories. These counts do not necessarily represent the number of events during a given season, as some events are represented by more than one sounding (e.g., the three proximity soundings for the fall SIGWIND category are all associated with the same 23 September 2003 event). Additionally, a wide variety of sample sizes exists seasonally, leading to a

TABLE 4. As in Table 3 (without Sig wind), but for 700–500-mb lapse rate.

	<i>P</i> value	Mean value of 700–500-mb lapse rate ( $^{\circ}\text{C km}^{-1}$ )
1–10	<0.001	5.99
11–50	<0.001	6.02
51–100	<0.001	6.01
101+	N/A	6.44

substantial meteorological summer dataset, but a markedly smaller sample size among other the seasons. For example, during the winter, individual samples were relatively small, such that SIGWIND and 101+ were combined into a single category. While this approach leads to the greater representation of some events relative to other events, it allows us to maximize the degree of sampling of each environment supporting the severe storms.

Before additional analysis is presented, we note that the prognostic utility of any individual parameter is limited, as discussed in Doswell and Schultz (2006). Such parameters represent measurements of the near-storm environment for northeast U.S. severe storms and, thus, provide diagnostic guidance. Holistic analysis of the temporal and spatial variations in the evolution of the

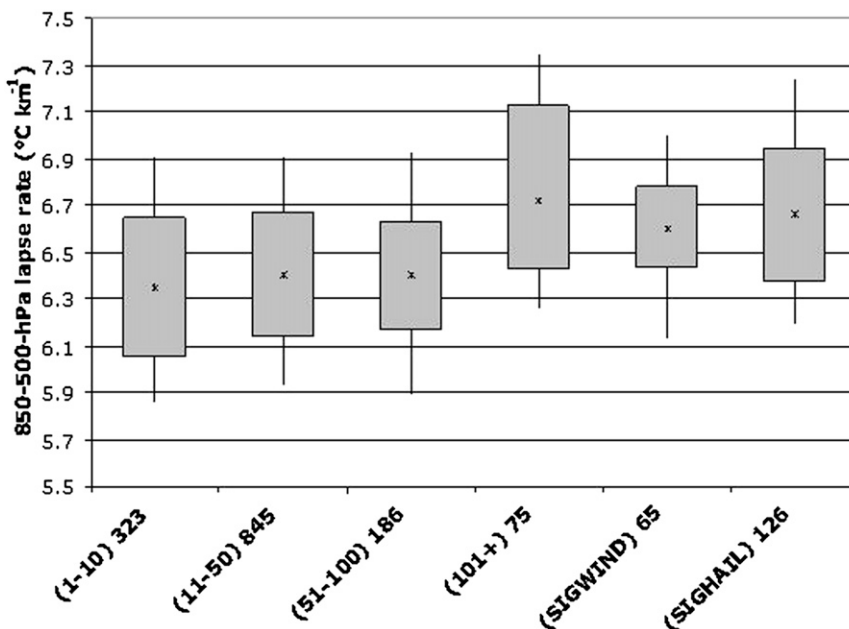


FIG. 9. Box-and-whiskers plots for summer 850–500-hPa lapse rate. The ends of the solid boxes represent the 25th and 75th percentiles of the distribution with the ends of the whiskers representing the 10th and 90th percentiles of the distribution and asterisks depicting distribution medians. Sample sizes (corresponding to the number of sounding observations considered) are listed beside event categories along the abscissa.

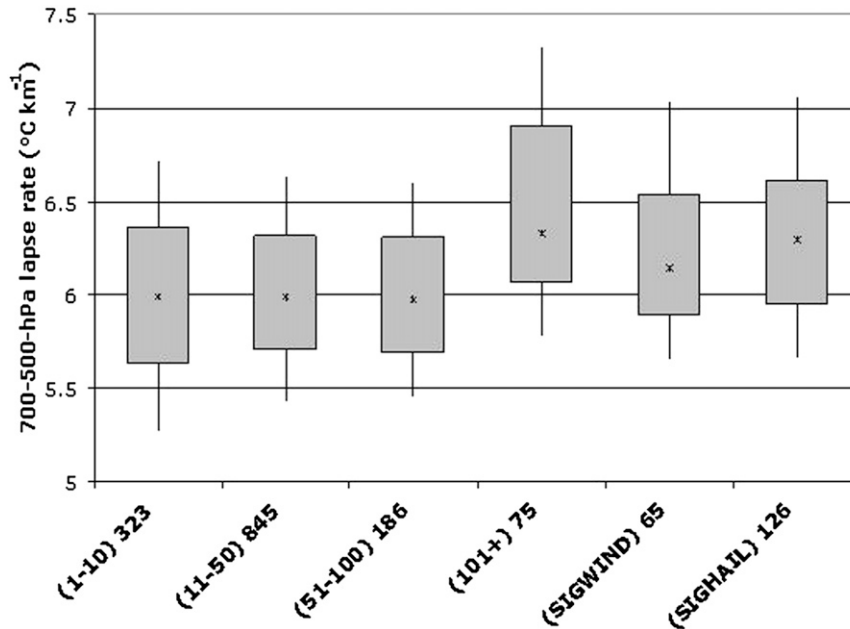


FIG. 10. As in Fig. 9, but for the 700–500-hPa lapse rate.

atmosphere is needed to create a more accurate forecast.

To quantify the differences among the meteorological parameters in the various classes of event magnitudes, we employed a two-tailed Student's *t* test assuming unequal variances (Wilks 2006). In doing so, variables were analyzed within their various event magnitude classes and were paired between differing classes. Upon pairing, a *P* value was determined, that quantifies the ability of a parameter to distinguish between various event magnitudes.

## 2) RESULTS

Among the vast array of parameters considered, and the multitude of pairings investigated, very few pairings yield both 1) statistical significance and 2) conceptual meaning for operational purposes. It would be highly unwieldy and without physical meaning to provide every possible combination across all categories and seasons. Thus, only selected pairings are presented.

Figure 8 summarizes several parameters that discriminate between pairings of event magnitudes at a *P*-value threshold of 0.05, and is used as the basis for further discussion of pairings during the summer. Among these, the 850–500- and 700–500-hPa lapse rates (related to 500-hPa temperatures) appear to discriminate well between the 101+-report class and other events (Tables 3 and 4 and Figs. 9 and 10). Steeper midlevel lapse rates can be associated with the enhanced potential for stronger convection, should initiation occur.

There is also a notable signal for stronger MLCIN to be present for the 101+ category compared to the lower-end events during the summer, as illustrated in Table 5. The convective inhibition acts to delay convective initiation until large-scale ascent, as discussed in the pattern analysis section, while surface heating and orographic influences assist in the eventual convective development and vigor. However, it should be noted that the stronger MLCIN for the 101+-category events may merely reflect the stable nocturnal boundary layer, with the majority of these events having been represented by 1200 UTC soundings (Table 1). In rare instances, the stronger MLCIN may indicate the presence of an elevated mixed layer (EML) if the parcels originate within the mixing layer of a hot and dry desert region. Substantial events have been noted in association with an EML being advected across the Northeast (Farrell and Carlson 1989; Johns and Dorr 1996; Banacos and Ekster 2010) and can be an important distinction when examining the source of the convective inhibition. Evidence of an EML could be investigated through inspection of

TABLE 5. As in Table 3 (without Sig wind), but for MLCIN.

	<i>P</i> value	Mean value of MLCIN ( $\text{J kg}^{-1}$ )
1–10	0.001	–67
11–50	<0.001	–62
51–100	0.002	–70
101+	N/A	–98

TABLE 6. As in Table 3 (without Sig wind), but for DCAPE.

	<i>P</i> value	Mean value of DCAPE ( $\text{J kg}^{-1}$ )
1-10	N/A	639
11-50	<0.001	756
51-100	<0.001	784
101+	<0.001	935

thermodynamic profiles aloft on a case-by-case basis. Such a consistent signal across the various categories is again not noted for other seasons for MLCIN.

Likewise, DCAPE (Gilmore and Wicker 1998) is found to be a valuable parameter in distinguishing between the 101+-report class and other report classes (Table 6 and Fig. 11). DCAPE involves comparisons between the temperature profile of a theoretical air parcel descending while following the trace of a saturated adiabat with the low-level environmental temperature profile. It shows skill in predicting the numbers of reports, perhaps as a result of its direct quantification of downward buoyancy given a downdraft and its relationship to downdraft strength. The lack of statistically significant pairings during other seasons precludes additional discussion for non-summer periods.

Various measures of CAPE (e.g., mixed-layer CAPE or most unstable CAPE) and vertical wind shear describe storm intensity and the severe weather threat (e.g., Brooks and Craven 2002; Johns and Doswell 1992). However, these variables, as well as many other variables,

are not found to distinguish between the various classes of report quantities (e.g., Figs. 12 and 13). Despite not being statistically significant, it should be noted that MLCAPE experiences a general rise in magnitude with increasing event magnitude for summer events, with the greatest separation between events featuring at least 101+ reports and those producing fewer reports. However, report quantities are likely more intimately related to other factors, such as the size of the warm sector and the spatial distribution of the parameters rather than the individual magnitudes of the parameters measured from specific soundings. The broad area over which proximity sounding parameters were calculated may also limit statistical significance. Furthermore, the proximity soundings did not typically sample the environments at the peaks of the severe weather episodes. As a result, variables relatively more influenced by boundary layer heating did not represent the inflow actually supporting the severe storms. The lack of statistical significance is even more marked outside of the summer (Fig. 8), when sample sizes within various event classes are smaller. As such, the following discussion presents spatial patterns and geometries to be considered in tandem with the observed radiosonde data, thus providing additional representation of convective weather environments across the Northeast.

*c. Pattern analysis*

In this section, composite images created using NARR data corresponding to the selected sounding

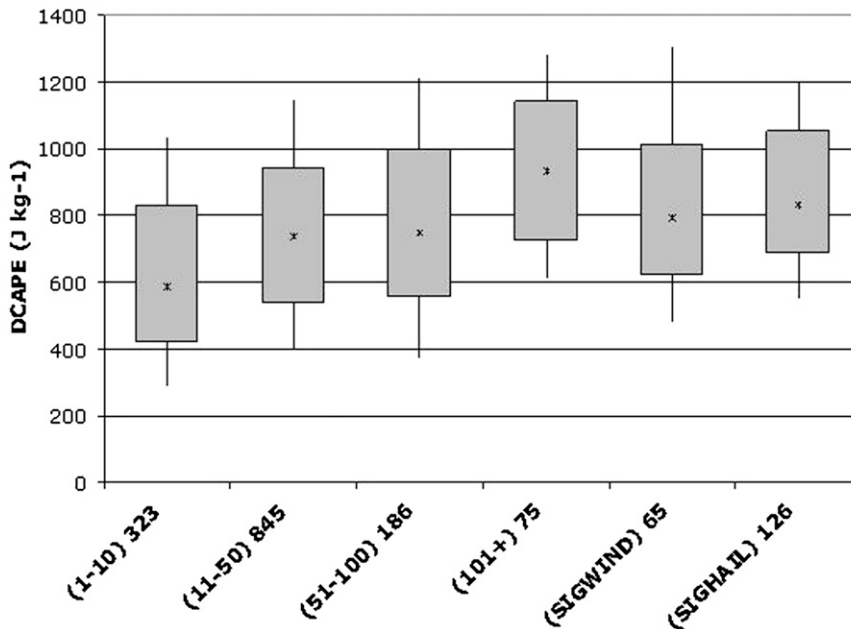


FIG. 11. As in Fig. 9, but for DCAPE.

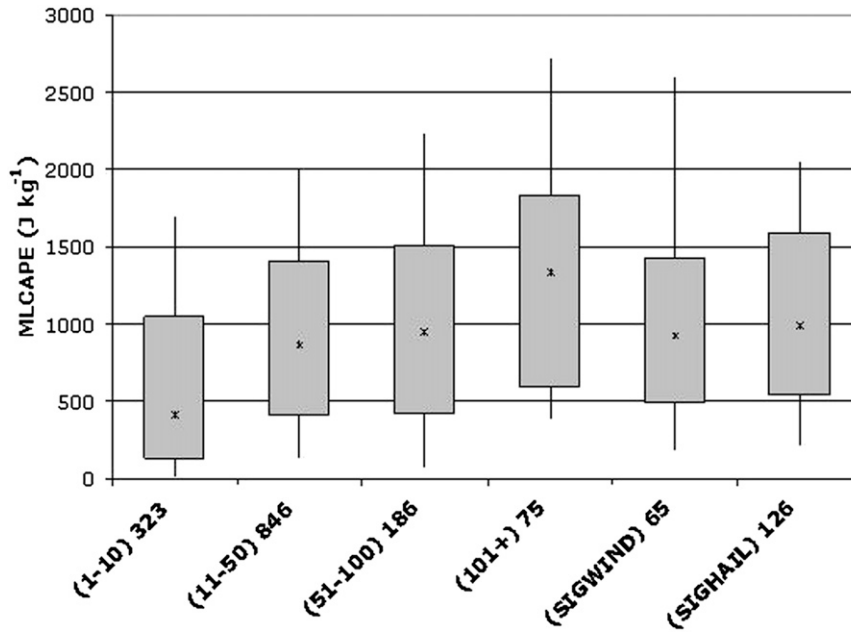


FIG. 12. As in Fig. 9, but for MLCAPE.

times are discussed. Given the operational and statistical significance of low- to midlevel lapse rates in distinguishing between event report magnitudes, the present section is primarily focused on 500- and 850-hPa mass, momentum, and thermodynamic fields, with a more peripheral discussion on other notable pattern differences.

1) SUMMER (JUNE–AUGUST)

Similar 500-hPa patterns are evident between the subsets, with a ridge centered on the Southwest dominating much of the interior western and central states, while an eastern trough is centered on Hudson Bay (Fig. 14). Consistent with these results, Banacos and

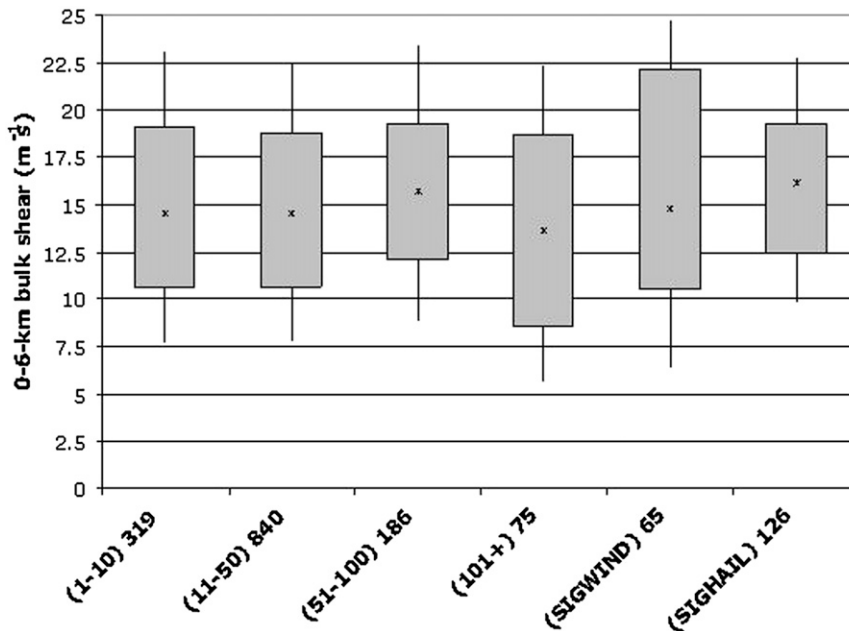


FIG. 13. As in Fig. 9, but for the 0–6-km bulk shear.

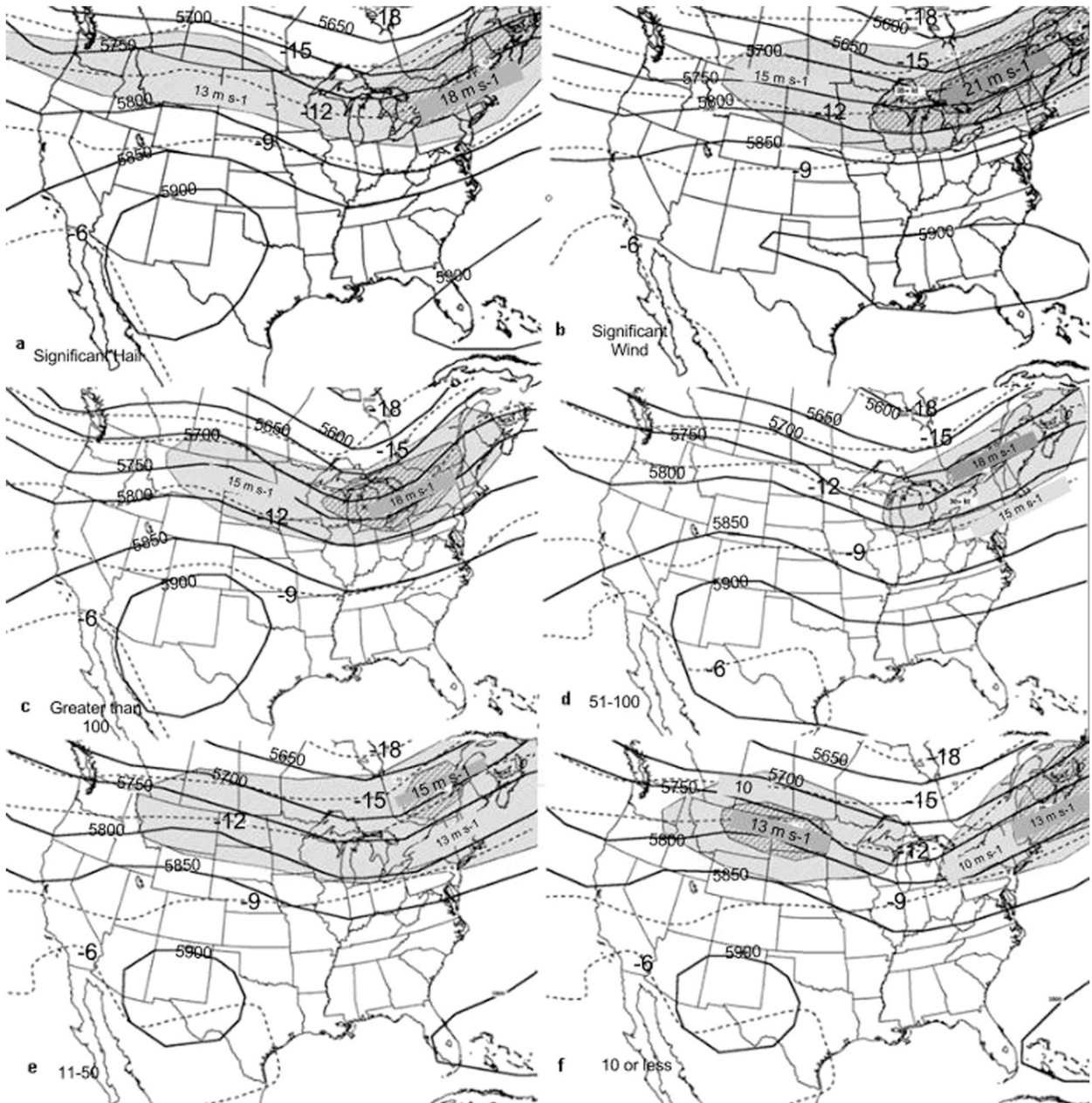


FIG. 14. Composite 500-hPa values for summer events: (a) significant hail, (b) significant wind, (c) >100 reports, (d) 51–100 reports, (e) 11–50 reports, and (f) 10 reports. Solid lines represent geopotential heights; dashed lines, temperature ( $^{\circ}\text{C}$ ); and hatched area, wind speeds in  $\text{m s}^{-1}$ .

Ekster (2010) have found that, specifically in north-eastern United States cases where an EML enhances convection, a negative midlevel height anomaly is located over the northern Great Lakes. However, differences arise with the tilt, with a deeper and more negatively tilted trough apparent in the significant hail and >100 reports composites (Figs. 14a,c). In the presence of negatively tilted troughs, midlatitude wave amplification

(e.g., Bluestein 1993) supports enhanced convective activity (Glickman et al. 1977). The higher-report events likely, in part, reflect the positioning of the mid- to upper trough such that convective initiation and vigor is favored over more populated coastal and metropolitan areas. Meanwhile, the significant wind event composite illustrates a tight 500-hPa height gradient and associated strong westerly flow (Fig. 14b).

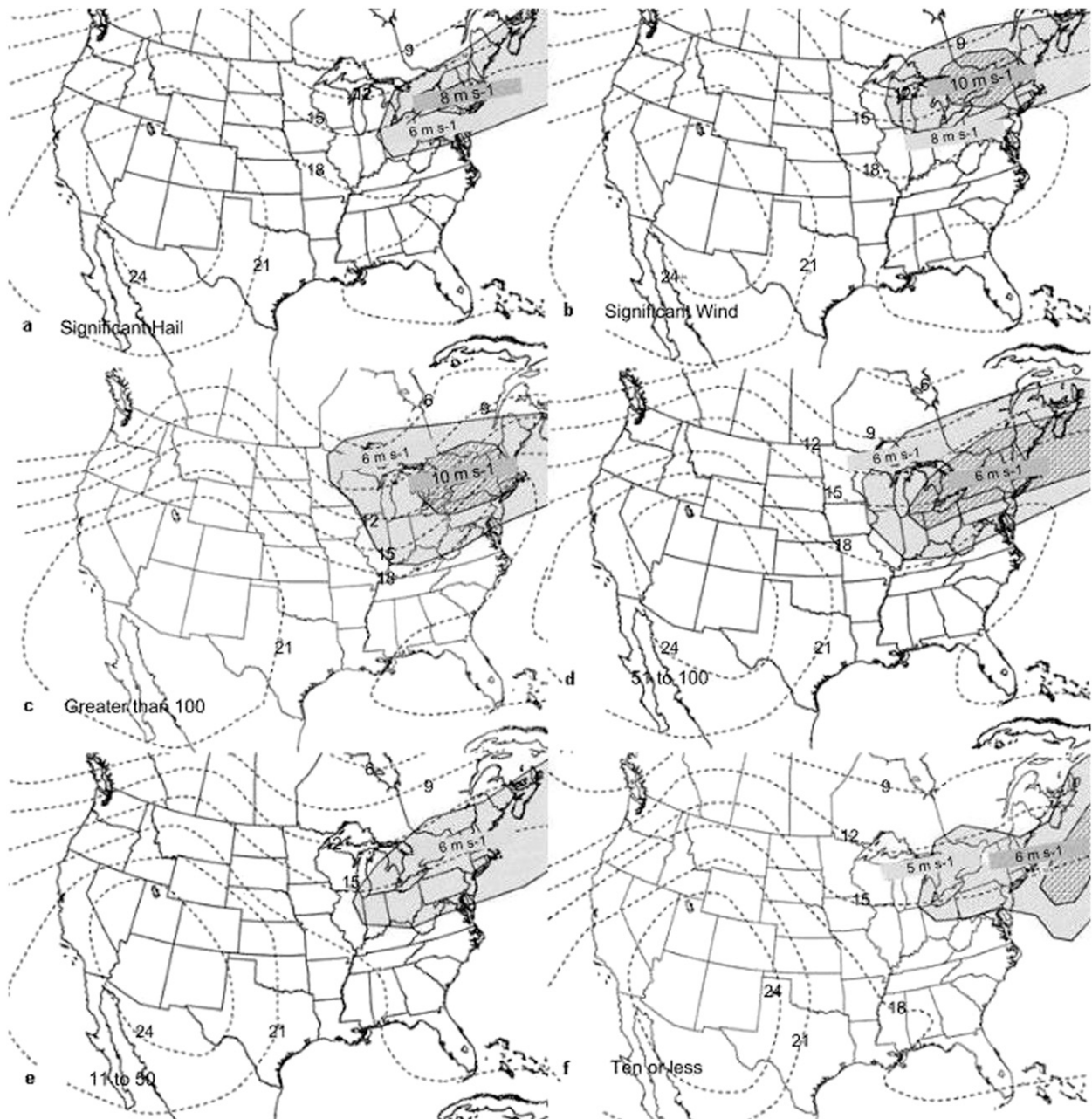


FIG. 15. As in Fig. 14, but for 850 hPa.

However, it is important to note that individual radiosonde observations over the United States may not fully sample the kinematic characteristics of the jet-enhancing convection if the jet resides north of the international border, which is common during the summer owing to the northward migration of the jet (Fig. 14). As such, a holistic, regional-scale analysis is encouraged in assessing severe weather potential.

The position of the mid- and upper-level jet maximum does appear to be operationally meaningful (Fig. 14), as

the right-entrance region and curvature downstream of the trough enhance upward motion via upper-level divergence (Keyser and Shapiro 1986). Conversely, upper-level convergence is present within the right-exit region of the jet, though the associated augmentation of 0–3-km SRH, its collocation with surface convergence, and the warm sector can compensate, making severe weather reports common in the right-exit as well as the right-entrance regions (Clark et al. 2009).

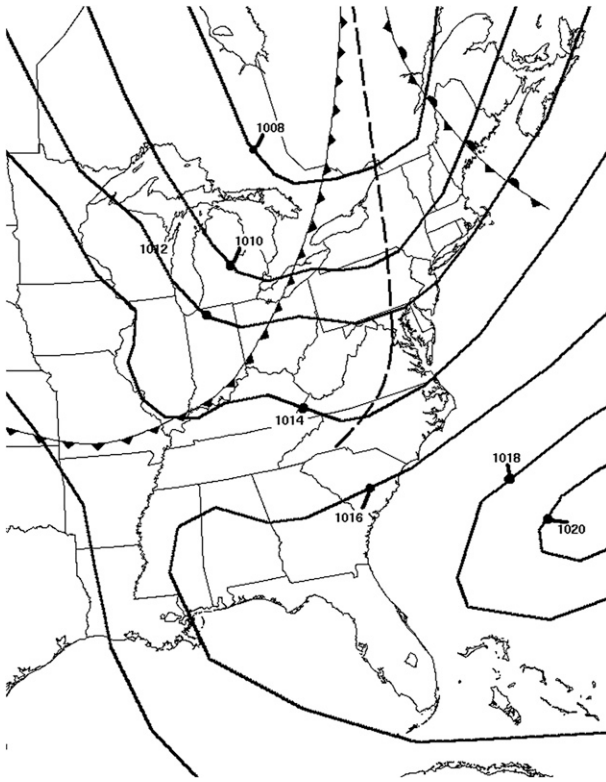


FIG. 16. Composite sea level pressure and frontal analysis for summer events with >100 reports. Solid lines are isobars (hPa).

Furthermore, the zone of enhanced mid- and upper-level flow is collocated with stronger lower-tropospheric winds (Figs. 15a–c). These lower-tropospheric winds, in turn, promote differential thermal and moisture advection, yielding increased convective instability (e.g., Uccellini and Johnson 1979).

Not surprisingly, the mid- and upper-level trough is progressively more neutrally to positively tilted and less amplified for the lower-report subsets (Figs. 14d–f), compared to the slight negative tilt of the greater-report events. Weaker speeds attendant to the low-level jet are evident for the lower-report cases (Figs. 15d–f). The position of the mid- and upper-level jet is also found to be displaced downstream of that for the more prolific report days (Figs. 14d–f).

The 850-hPa analysis for the more prolific report events shows a thermal ridge extending northward along the coast into southern New England, which was also noted by Johns and Dorr (1996), and may be associated with enhanced convective inhibition (Figs. 15a–c). However, an appreciable difference is noted at 850 hPa in the less-than-10-report subset (Fig. 15f), with no apparent thermal ridge, suggesting weaker low- to-midlevel lapse rates.

Finally, composite surface data for the >100-report subset reflect a low over west-central Quebec, with a prefrontal, Appalachians lee trough extending into the mid-Atlantic, and the primary surface front extending into southern Ontario southwestward into the mid-Mississippi River valley (Fig. 16).

## 2) SPRING (MARCH–MAY)

Similar to the significant severe and more prolific report events of the summer, an amplified, negatively tilted trough centered on Hudson Bay and favorably placed mid- to upper-level jets approaching the region appear to be supportive of convective development and sustenance (Figs. 17a–c). With the significant hail cases, a  $-18^{\circ}\text{C}$  isotherm reaching the Canadian–United States border overlaying warmer than climatologically normal low-level temperatures offers further support that lapse rates are important to significant hail formation in combination with favorable kinematics (Figs. 17a and 18a). For significant wind events, deep-layer, predominantly westerly flow is once again evident (Figs. 17b and 18b). A very limited dataset exists for events with greater than 100 reports, with the only case being 31 May 2002. However, the synoptic pattern for this particular event was quite similar to the prolific report events of the summer. Although the upper trough is rather amplified for the 51–100-report subset, it is displaced farther westward into the Midwest, lending further credence that the positioning of the trough relative to greater population may play a role in the final report count (Fig. 17c). Also similar to the summer groupings, the mid- and upper-level trough is progressively more neutrally to positively tilted and less amplified for the lower-report subsets (Figs. 17d,e). Low levels with the 51 or more reports and significant subsets are characterized by a thermal ridge along the coastal states (Figs. 18a–c). The low-level winds are also comparatively weaker for the lower report subsets (Figs. 18d,e).

## 3) FALL (SEPTEMBER–NOVEMBER)

Only one case of significant wind occurred in the fall, on 9 September 2003, so extreme caution should be used in assuming that the pattern data are representative of significant wind events. However, this particular event was portrayed as an uncharacteristically strong negatively tilted trough rotating into the eastern Great Lakes region (not shown). Reports were primarily clustered along coastal regions across New Jersey and New York.

A similar mid- and upper-level jet structure exists between the 11–50-report subset and the fewer-than-10 subset with a jet noted from the mid-Mississippi River valley into western portions of the Northeast, and a secondary jet exiting into the Gulf of St. Lawrence (not



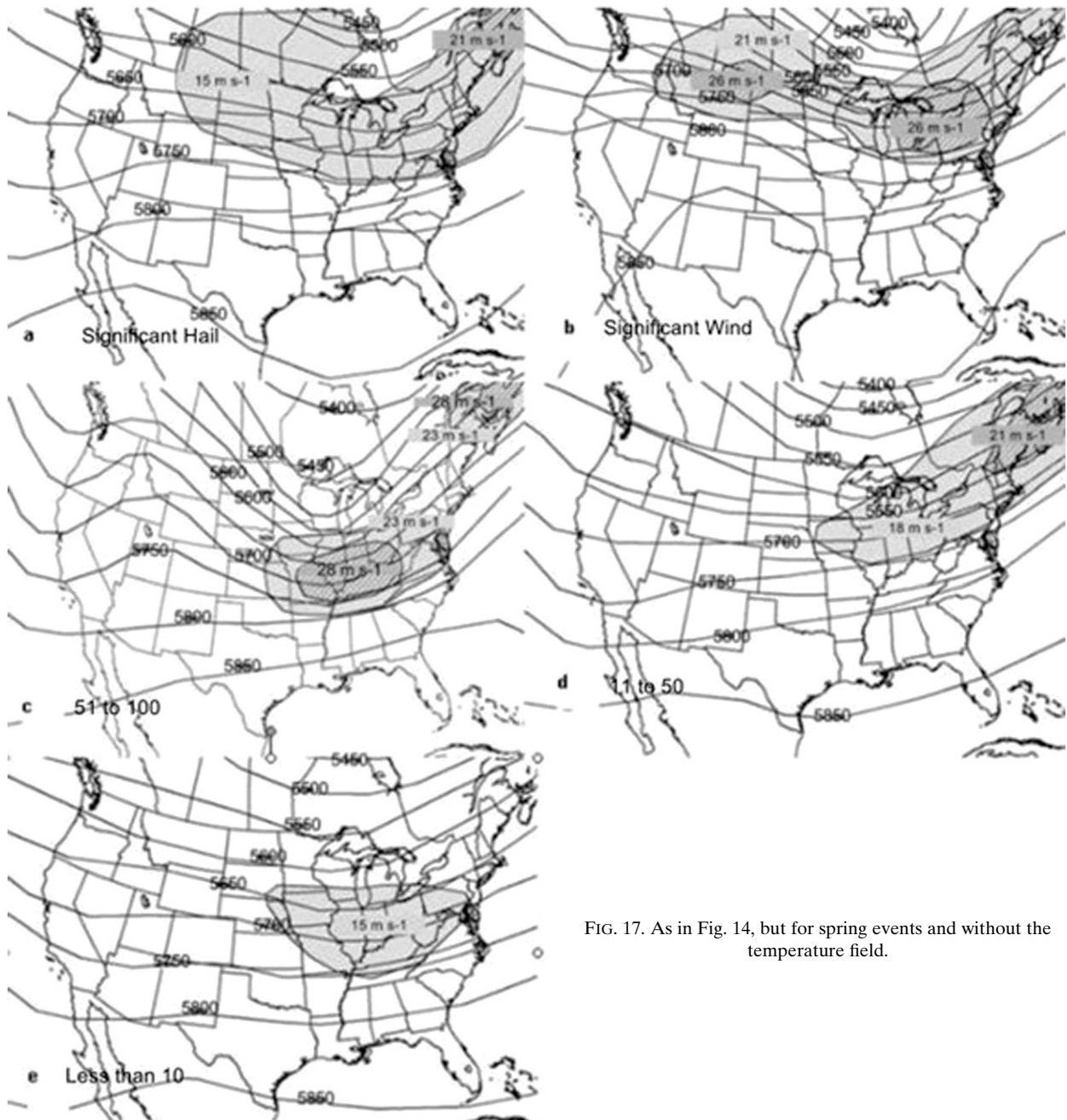


FIG. 17. As in Fig. 14, but for spring events and without the temperature field.

shown). A slightly negatively tilted to neutral upper trough extends from the Hudson Bay through the Great Lakes region for the higher-report dataset, while a much broader trough is evident over central Canada into the central Great Lakes for the fewer-than-10-report subset. In the low levels, the attendant jet winds are stronger for the 11–50-report subset (Fig. 19) compared to the fewer-than-10-report dataset (not shown).

At 850 hPa, the fewer-than-10-report subset features a weak thermal gradient northward along the Atlantic

coast, with the 10°–12°C isotherm impinging on western portions of the Northeast, whereas the 6°C isotherm resides across the same region in the 11–50 subset (Fig. 19). A 12°–15°C isotherm extends northward through the upper mid-Atlantic coast into southern New England for both subsets (Fig. 19).

#### 4) WINTER (DECEMBER–FEBRUARY)

While it may be inferred that vertical shear generally is too strong to support sustained updrafts, the limited

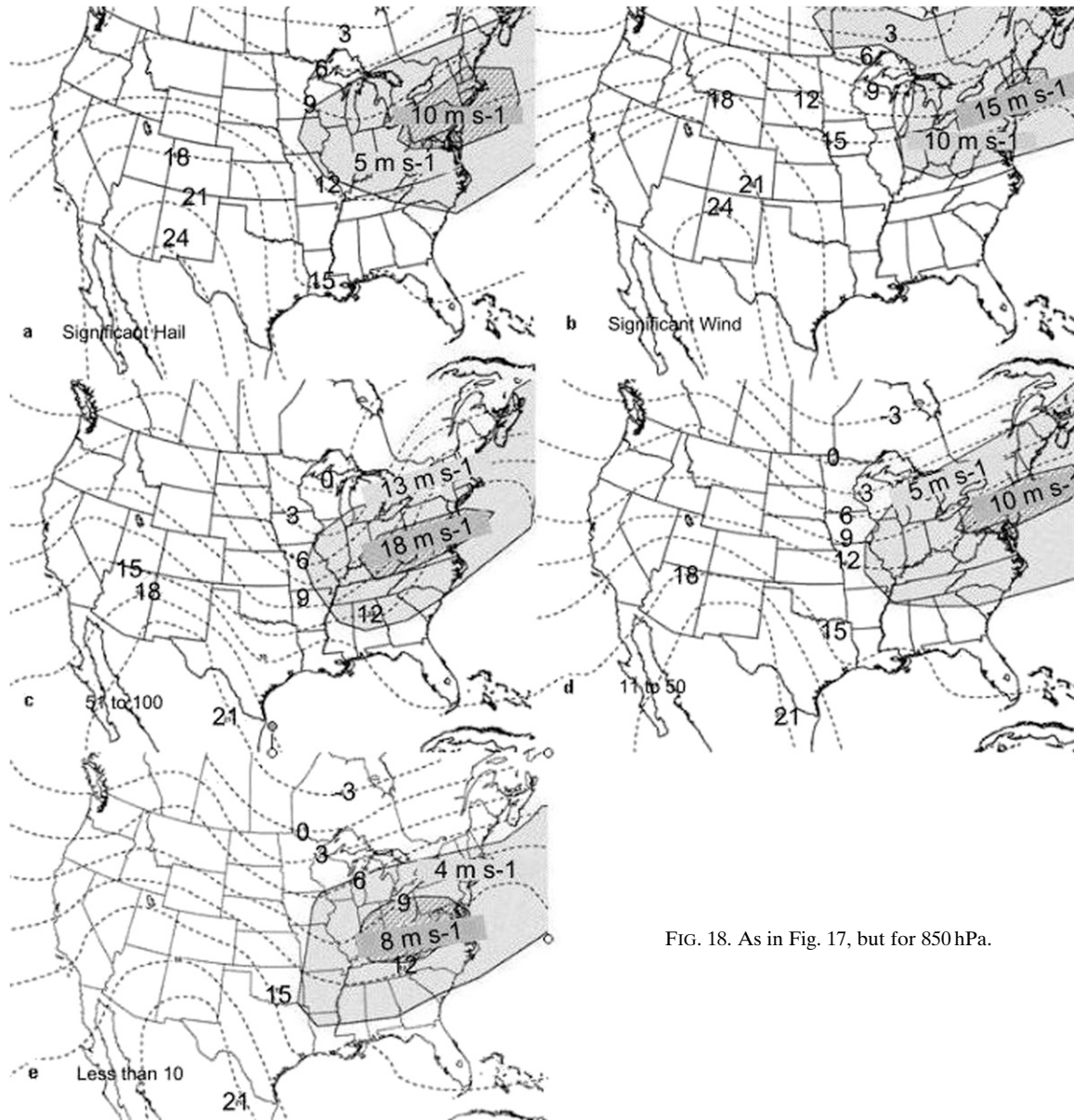


FIG. 18. As in Fig. 17, but for 850 hPa.

winter datasets reflect that favorable mid- and upper-level jet dynamics contribute to upward motion and the development of severe storms, despite limited instability. Similar patterns exist between the subsets, with an exiting jet in northern New England into New Brunswick, the Gulf of St. Lawrence, far eastern Quebec, Newfoundland, and Labrador (Fig. 20). A separate mid- to upper-level jet is approaching the Northeast, with the exact placement of the jet varied between the datasets. Nonetheless, a double-jet feature, with the favored left-exit region of the approaching jet and the right-entrance region of the exiting jet, appears to contribute to vertical motion across the region with all three subsets. One notable difference between the higher-end events, including

the one that produced over 100 reports and the significant wind event, is that the 850-hPa temperatures appear to be much warmer than the climatological normal in advance of the front (Fig. 21). Thus, the antecedent air mass is an important predictor as to whether widespread damaging winds can develop as convection increases. Anomalously warm/moist low levels should be noted as being operationally meaningful when forecasting severe potential in the winter.

#### 4. Conclusions

Relationships between the lower- and upper-air patterns and the magnitude of severe thunderstorm reports

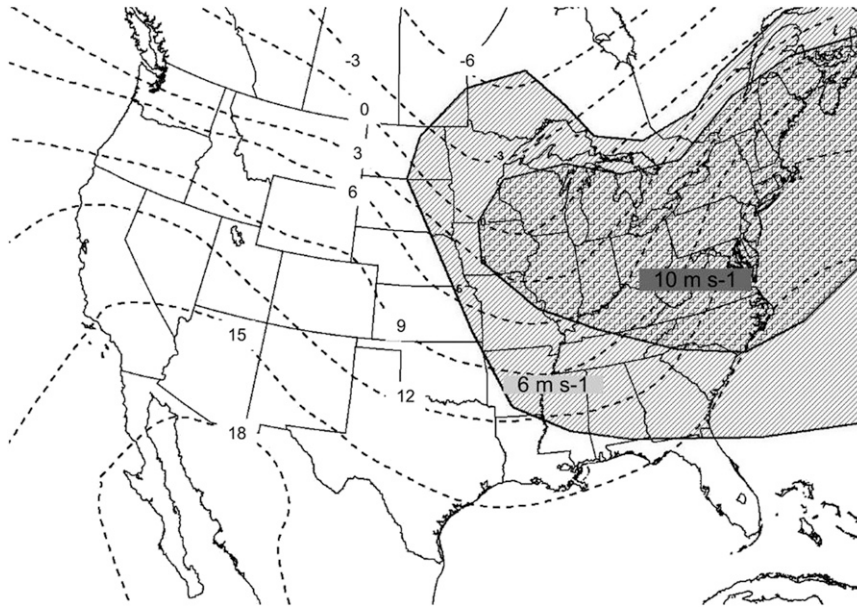


FIG. 19. Composite 850-hPa temperature ( $^{\circ}\text{C}$ , dashed) and wind (shaded,  $\text{m s}^{-1}$ ) for fall events with 11–50 reports.

across the northeastern United States were investigated. Given the high economic and social impacts of these events, it is of value to investigate these relationships to enhance forecaster awareness of the synoptic-scale patterns and the observed sounding data associated with them. In addition to event magnitude stratification, the

data were further separated by season, which reveal seasonal variations between the strength of forcing for deep, moist convection.

Following the examination of a large sample of observed radiosonde data, a few parameters were highlighted as having exhibited statistical significance in

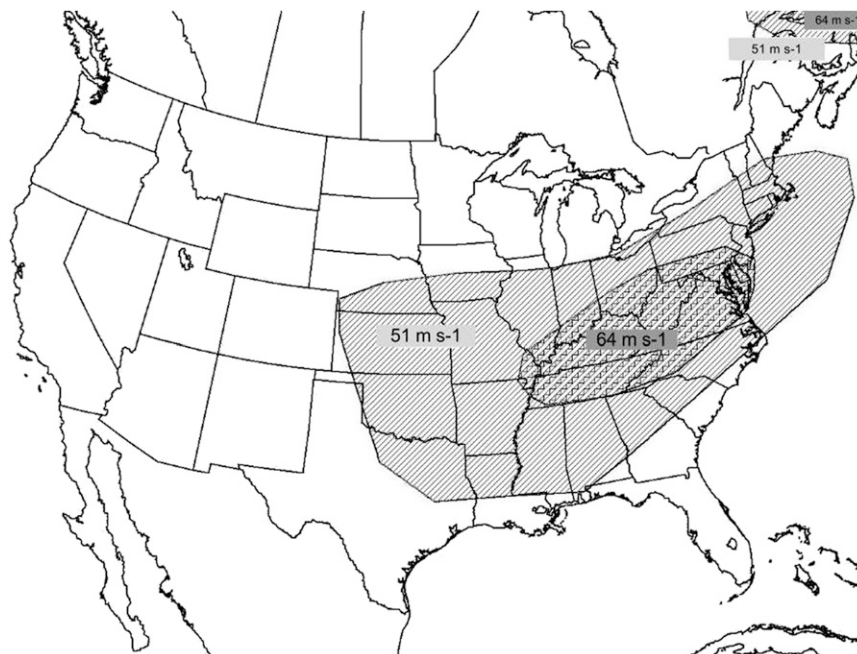


FIG. 20. Example of a double-upper-level jet structure shown with a composite 250-hPa wind (shaded,  $\text{m s}^{-1}$ ) for winter events with  $>100$  reports.

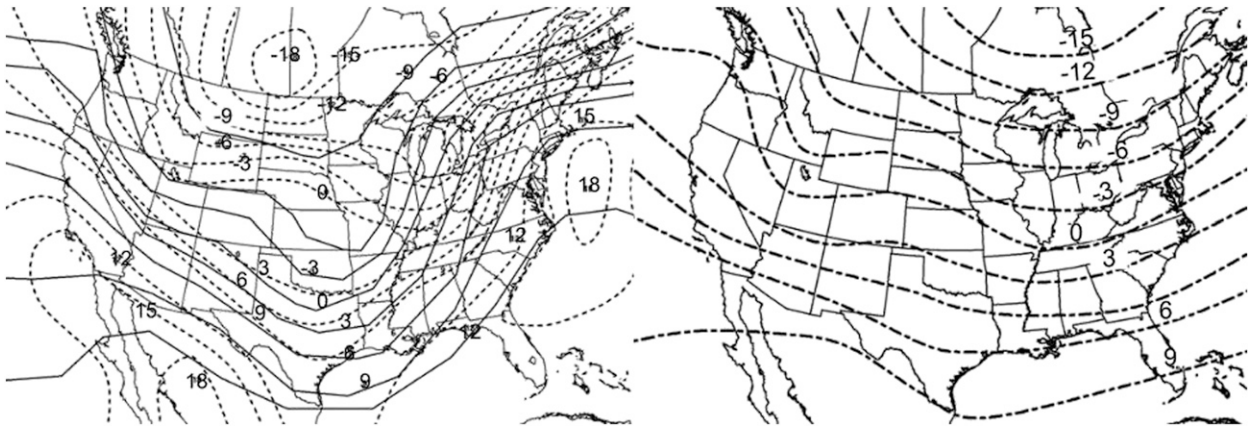


FIG. 21. The 850-hPa temperatures ( $^{\circ}\text{C}$ ) for winter events. (left) Dashed lines show an event with  $>100$  reports and solid lines show the composite temperature for significant wind events. (right) Climatological winter values for the same parameters during the study period.

discriminating between the various classes of report magnitude. While many parameters offer little discriminatory power among the various classes, the presence of relatively cool midlevel temperatures overlaying warm low-level air (i.e., steep low- to midlevel lapse rates), MLCIN and DCAPE appear to provide some separation between the most substantial report categories (101+) and other categories during the summer.

Composite patterns constructed using NARR data provide spatial analyses on basic mass, momentum, and thermodynamic fields, which can aid in pattern recognition for prognostic and diagnostic purposes. Among other findings, greater amplification to the midlevel pattern is noted in the higher-end events, with stronger mid- and upper-level flow noted within a jet that offers enhanced forcing for vertical motion. This vertical motion was particularly noteworthy during the winter, when a double-structured jet was evident. The tilt of a nearby midlevel trough appears to exhibit some utility in identifying patterns more supportive of greater-report-producing convection. At the surface, the pattern typically reveals a prefrontal trough, or a similar feature east of the Appalachians, with a cold front associated with the midlevel trough.

Spatial patterns and geometries presented in this paper can be considered in tandem with the observed radiosonde data to provide a more quantitative estimate of the convective threat across the Northeast. Future work may investigate the relationship between these findings and local topographic variations, an endeavor for which high-resolution, mesoscale modeling may play a useful role.

*Acknowledgments.* The authors thank Stephen Corfidi, Richard Thompson, and Philip Schumacher, as well as two anonymous reviewers, whose comments led to

significant improvements to the manuscript. We would also like to dedicate the manuscript to Jonathan Racy, whose enthusiasm, encouragement, and optimism will never be forgotten at the Storm Prediction Center.

#### REFERENCES

- Anderson, C. J., C. K. Wikle, Q. Zhou, and J. A. Royle, 2007: Population influences on tornado reports in the United States. *Wea. Forecasting*, **22**, 571–579.
- Banacos, P. C., and M. L. Ekster, 2010: The association of the elevated mixed layer with significant severe weather events in the northeastern United States. *Wea. Forecasting*, **25**, 1082–1102.
- , —, J. Dellicarpini, and E. Lyons, 2012: A multiscale analysis of the 1 June 2011 northeast U.S. severe weather outbreak and associated Springfield, Massachusetts tornado. *Electron. J. Severe Storms Meteor.*, **7** (7). [Available online at <http://www.ejssm.org/ojs/index.php/ejssm/article/view/105>.]
- Bluestein, H. B., 1993: *Observations and Theory of Weather Systems*. Vol. II, *Synoptic–Dynamic Meteorology in Midlatitudes*, Oxford University Press, 594 pp.
- Bosart, L. F., K. LaPenta, A. Seimon, M. Dickinson, and T. J. Galarneau Jr., 2004: Terrain-influenced tornadogenesis in the northeastern United States. Preprints, *11th Conf. on Mountain Meteorology and the Annual Mesoscale Alpine Program (MAP)*, Bartlett, NH, Amer. Meteor. Soc., 17.3. [Available online at <https://ams.confex.com/ams/pdfpapers/77126.pdf>.]
- Brooks, H. E., and J. P. Craven, 2002: A database of proximity soundings for significant severe thunderstorms, 1957–2003. Preprints, *21st Conf. on Severe Local Storms*, San Antonio, TX, Amer. Meteor. Soc., 16.2. [Available online at [https://ams.confex.com/ams/SLS\\_WAF\\_NWP/techprogram/paper\\_46680.htm](https://ams.confex.com/ams/SLS_WAF_NWP/techprogram/paper_46680.htm).]
- Clark, A. J., C. J. Schaffer, W. A. Gallus Jr., and K. Johnson-O'Mara, 2009: Climatology of storm reports relative to upper-level jet streaks. *Wea. Forecasting*, **24**, 1032–1051.
- Doswell, C. A., III, and D. M. Schultz, 2006: On the use of indices and parameters in forecasting severe storms. *Electron. J. Severe Storms Meteor.*, **1** (3). [Available online at <http://www.ejssm.org/ojs/index.php/ejssm/article/viewArticle/11/12>.]
- , H. E. Brooks, and M. P. Kay, 2005: Climatological estimates of daily local nontornadic severe thunderstorm probability for the United States. *Wea. Forecasting*, **20**, 577–595.

- Environmental Research Services, 2008: RAOB—The Universal Rawinsonde Observation program: Users guide and technical manual. ERS, 175 pp. [Available from Environmental Research Services, Matamoras, PA 18336 and online at [http://www.raob.com/user\\_manual.php](http://www.raob.com/user_manual.php).]
- Evans, J. E., K. Carusone, M. M. Wolfson, M. Robinson, E. R. Ducot, and B. Crowe, 2004: Improving convective weather operations in highly congested airspace with the Corridor Integrated Weather System (CIWS). Preprints, *11th Conf. on Aviation, Range and Aerospace Meteorology*, Hyannis, MA, Amer. Meteor. Soc., P1.5. [Available online at <https://ams.confex.com/ams/pdfpapers/81276.pdf>.]
- Farrell, R. J., and T. N. Carlson, 1989: Evidence for the role of the lid and underrunning in an outbreak of tornadic thunderstorms. *Mon. Wea. Rev.*, **117**, 857–871.
- Gilmore, M. S., and L. J. Wicker, 1998: The influence of mid-tropospheric dryness on supercell morphology and evolution. *Mon. Wea. Rev.*, **126**, 943–958.
- Glickman, T. S., N. J. Macdonald, and F. Sanders, 1977: New findings on the apparent relationship between convective activity and the shape of 500 mb troughs. *Mon. Wea. Rev.*, **105**, 1060–1061.
- Hales, J. E., Jr., 1988: Improving the watch/warning program through use of significant event data. Preprints, *15th Conf. on Severe Local Storms*, Baltimore, MD, Amer. Meteor. Soc., 165–168.
- Hart, J. A., J. Whistler, R. Lindsay, and M. Kay, 1999: NSHARP, version 3.10. Storm Prediction Center, National Centers for Environmental Prediction, Norman, OK, 33 pp.
- Johns, R. H., and C. A. Doswell III, 1992: Severe local storms forecasting. *Wea. Forecasting*, **7**, 588–612.
- , and R. A. Dorr Jr., 1996: Some meteorological aspects of strong and violent tornado episodes in New England and eastern New York. *Natl. Wea. Dig.*, **20** (4), 2–12.
- Keyser, D., and M. A. Shapiro, 1986: A review of the structure and dynamics of upper-level frontal zones. *Mon. Wea. Rev.*, **114**, 452–499.
- LaPenta, K. D., L. F. Bosart, T. J. Galarneau Jr., and M. J. Dickinson, 2005: A multiscale examination of the 31 May 1998 Mechanicville, New York, tornado. *Wea. Forecasting*, **20**, 494–516.
- Lericos, T. P., H. E. Fuelberg, M. L. Weisman, and A. I. Watson, 2007: Numerical simulations of the effects of coastlines on the evolution of strong, long-lived squall lines. *Mon. Wea. Rev.*, **135**, 1710–1731.
- Lombardo, K. A., and B. A. Colle, 2010: The spatial and temporal distribution of organized convective structures over the Northeast and their ambient conditions. *Mon. Wea. Rev.*, **138**, 4456–4474.
- , and —, 2011: Convective storm structures and ambient conditions associated with severe weather over the northeast United States. *Wea. Forecasting*, **26**, 940–956.
- Mesinger, F., and Coauthors, 2006: North American Regional Reanalysis. *Bull. Amer. Meteor. Soc.*, **87**, 343–360.
- Murray, J. C., and B. A. Colle, 2011: The spatial and temporal variability of convective storms over the northeast United States during the warm season. *Mon. Wea. Rev.*, **139**, 992–1012.
- Riley, G. T., and L. F. Bosart, 1987: The Windsor Locks, Connecticut tornado of 3 October 1979: An analysis of an intermittent severe weather event. *Mon. Wea. Rev.*, **115**, 1655–1677.
- Smith, B. T., A. C. Winters, C. M. Mead, A. R. Dean, and T. E. Castellanos, 2010: Measured severe wind gust climatology of thunderstorms for the contiguous United States, 2003–2009. Preprints, *25th Conf. Severe Local Storms*, Denver, CO, Amer. Meteor. Soc., 16B.3. [Available online at <https://ams.confex.com/ams/25SLS/webprogram/Paper175594.html>.]
- Trapp, R. J., D. M. Wheatley, N. T. Atkins, R. W. Przybylinski, and R. Wolf, 2006: Buyer beware: Some words of caution on the use of severe wind reports in postevent assessment and research. *Wea. Forecasting*, **21**, 408–415.
- Uccellini, L. W., and D. R. Johnson, 1979: The coupling of upper and lower tropospheric jet streaks and implications for development of severe convective storms. *Mon. Wea. Rev.*, **107**, 682–703.
- Wasula, A. C., L. F. Bosart, and K. D. LaPenta, 2002: The influence of terrain on the severe weather distribution across interior eastern New York and western New England. *Wea. Forecasting*, **17**, 1277–1289.
- Weiss, S. J., J. A. Hart, and P. R. Janish, 2002: An examination of severe thunderstorm wind report climatology: 1970–1999. Preprints, *21st Conf. on Severe Local Storms*, San Antonio, TX, Amer. Meteor. Soc., 11B.2. [Available online at <https://ams.confex.com/ams/pdfpapers/47494.pdf>.]
- Wilks, D. S., 2006: *Statistical Methods in the Atmospheric Sciences*. 2nd ed. Academic Press, 627 pp.